JACS
JOURNAL OF THE AMERICAN CHEMICAL SOCIETY

Article

pubs.acs.org/JACS

Uncovering Molecular Details of Urea Crystal Growth in the Presence of Additives

Matteo Salvalaglio,[†,‡] Thomas Vetter,[†] Federico Giberti,[‡] Marco Mazzotti,*[,†] and Michele Parrinello*[,‡,§]

[†]Institute of Process Engineering, ETH Zurich, CH-8092 Zurich, Switzerland

[‡]Department of Chemistry and Applied Biosciences, ETH Zurich, Zurich, Switzerland

[§]Facoltà di Informatica, Istituto di Scienze Computazionali, Università della Svizzera Italiana Via G. Buffi 13, 6900 Lugano Switzerland

Supporting Information

ABSTRACT: Controlling the shape of crystals is of great practical relevance in fields like pharmacology and fine chemistry. Here we examine the paradigmatic case of urea which is known to crystallize from water with a needle-like morphology. To prevent this undesired effect, inhibitors that selectively favor or discourage the growth of specific crystal faces can be used. In urea the most relevant faces are the {001} and the {110} which are known to grow fast and slow, respectively. The relevant growth speed difference between these two crystal faces is responsible for the needle-like structure of crystals grown in water solution. To prevent this effect, additives are used to slow down the growth of one face relative to another, thus controlling the shape of the crystal. We study the growth of fast {001} and slow {110} faces in water solution and the effect of shape controlling inhibitors like biuret. Extensive sampling through molecular dynamics simulations provides a microscopic picture of the growth mechanism and of the role of the additives. We find a continuous growth mechanism on the {001} face, while the slow growing {110} face evolves through a birth and spread process, in which the rate-determining step is the formation on the surface of a two-dimensional crystalline nucleus. On the {001} face, growth inhibitors like biuret compete with urea for the adsorption on surface lattice sites; on the {110} face instead additives cannot interact specifically with surface sites and play a marginal sterical hindrance of the crystal growth. The free energies of adsorption of additives and urea are evaluated with advanced simulation methods (well-tempered metadynamics) allowing a microscopic understanding of the selective effect of additives. Based on this case study, general principles for the understanding of the anisotropic growth of molecular crystals from solutions are laid out. Our work is a step toward a rational development of novel shape-affecting additives.

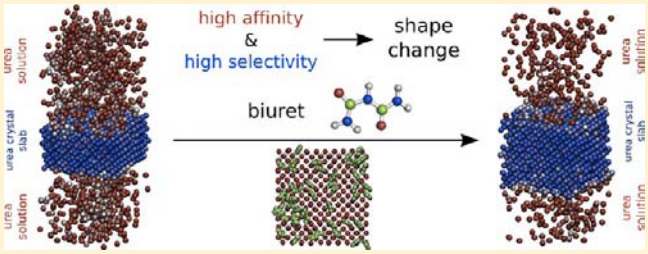

INTRODUCTION

The size and shape of crystals play a crucial role in chemical and pharmaceutical manufacturing.[1] Most drugs are purified and sold as crystalline solids, and thus their size and shape have a direct impact on the efficiency of the production processes. Furthermore, recent experiments have demonstrated that the crystalline form of a drug plays a role in its activity, affecting its dissolution kinetics,[2] its bioavailability,[3] and its uptake performances.

The appearance of needle or platelet crystals is the unwelcome outcome of different growth rates of different crystal faces. This phenomenon involves a wide range of length scales going from the molecular detail, that determines the intrinsic physical chemical reasons of the anisotropic growth, to the macroscopic scale, where the shapes of the growing crystallites can be observed and monitored with experimental techniques. The growth can be controlled either by acting on the macroscopic operative conditions[4−6] or by employing additives capable of hindering the growth of crystals at the molecular scale.[7,8] The effect of the interaction of the additives with the growing crystallites is the selective enhancement or discouragement of crystal growth on specific faces, which can be used to reduce differences in growth rates of individual crystal faces and thereby reduces anisotropic growth. Despite numerous examples in the literature showing the effectiveness of this approach,[9−14] the design of growth inhibition strategies lacks in rational and determinisitc strategies, relying on the contrary on empirical approaches and on trial and error.

Given the increasing computational power and the development of algorithms and methods for enhanced sampling, molecular modeling is emerging as a viable approach toward building a comprehensive picture of molecular phenomena involved in crystallization processes.[15] In this paper we illustrate this capability by performing standard and enhanced sampling molecular dynamics (MD) simulations of the surface growth of urea and its interaction with different additives. More specifically a full atomistic description of the surface dynamics and thermodynamics of the fast {001} and slow {110} growing faces is provided.

Received: July 27, 2012
Published: September 19, 2012

dx.doi.org/10.1021/ja307408x | J. Am. Chem. Soc. 2012, 134, 17221−17233

We have chosen urea for a number of reasons: It shows fast kinetics of nucleation and growth, it grows from aqueous solution to form needle-like crystals that expose two well-defined crystal faces, and biuret, a subproduct of the urea synthesis, is reported in the literature as an effective shape-changing additive for urea itself.[16−18] Urea represents a valid benchmark system for molecular modeling studies since it provides all the features and challenges of molecular crystals while having a rather small size and a simple structure. Furthermore the molecular representation of the solid is straightforward as urea does not have polymorphs. Its space group is $P\bar{4}2_1m$ with $Z = 2$. Its growth from water and methanol solutions was recently modeled by Piana et al. through a combination of MD and kinetic Monte Carlo (KMC) simulations; this approach has enabled an accurate description of the shape of a growing crystal.[19,20] In this framework our work aims at complementing what was accomplished by Piana et al., by proposing an atomistic description of the crystal growth mechanism, and enhancing our current understanding of the mode of action of the additives. The molecular description of the effects of additives on crystal growth is a challenging topic that has seldom been tackled in the literature. In addition, the reported MD simulations[21−23] have explored only the very limited time scale of a few nanoseconds.

A conceptual attempt to the rationalization of the additive role during the nucleation stage was carried out by Anwar et al.[24] approaching the problem through the study of a model system of Lennard-Jones (LJ) spheres in water. The additives were also represented in a simplified way as LJ dimers.

It is well-known that the study of the homogeneous nucleation from the liquid phase is very challenging, since it occurs on a time scale inaccessible to molecular simulations and therefore requires special techniques to be observed. In the case of solids consisting of molecules, the situation is made even more complicated by the fact that the molecules have to orient themselves in a specific way for nucleation to occur.[25] Here we take a different approach: We assume that a crystal face has been formed and study its growth with and without additives. We observe that simulations in the hundreds of nanoseconds are needed to properly sample the events that characterize the crystal surface dynamics.

Moreover, in this work we use well-tempered (WT) metadynamics simulations to enhance the sampling of adsorption and desorption events, thus allowing for a quantitative estimation of the associated free energies for both urea and additives on each face. WT metadynamics is a state-of-the-art enhanced sampling MD technique of recent formulation which enables an efficient sampling of rare events and a convergent estimation of free energies. It is therefore well suited to tackle relevant problems in the field of crystallization, ranging from model systems to realistic ones. Nucleation as well as the formation of a solid/liquid interface in a LJ fluid,[26] the early stages of the calcium carbonate nucleation[27,28] as well as its complexation through the interaction with foreign molecules, such as polyacrylates[28,29] and ASP-rich peptides,[30] are some examples of such studies.

METHODS

Urea Force Field. Given the protein denaturation properties of urea and the interest of the biomolecular modeling community in its effects on protein unfolding dynamics, a variety of urea force fields are available in the literature.[31] Although in the biomolecular simulation community the most widely used urea force field is the OPLS/GROMOS, originally proposed by Duffy et al.[32] and extended by Van Gunsteren et al.,[33] in our case we have employed the AMBER force field for urea which relies on the generalized Amber force field (GAFF)[34,35] parametrization and enables a handy implementation of a fully compatible force field for the simulation of additives. The choice of the GAFF force field has been tested against a correct representation of the solid homogeneous phase, proving to adequately reproduce both the elementary cell parameters and the melting temperature of pure crystalline urea. The cell parameters were monitored in three independent MD simulations of the bulk crystalline phase. We did not observe distortion of the crystal structure, obtaining lattice constants ($a = 0.556$, $c = 0.467$ nm, and $c/a = 0.840$) in good agreement with the experimental ($a = 0.565$, $c = 0.468$ nm and $c/a = 0.842$).[36] The melting temperature was evaluated monitoring the stability of the solid/liquid interface during MD simulations at different temperatures for systems composed of liquid and crystalline urea in contact. The melting temperature was estimated to be within 400 and 420 K, in qualitative agreement with the experimental melting temperature of urea (406−408 K).

Additives Structure and Parametrization. In order to perform MD simulations of urea crystal growth in the presence of foreign molecules, force field parameters within the framework of the GAFF[34,35] have been derived for every additive. The relaxed molecular structure was obtained by density functional theory (DFT) structural optimization performed at the B3LYP/6-31G(d,p) level using the implicit integral equation formalism polarized continuum model (IEFPCM)[37] to consider the aqueous environment. The partial atomic charges were computed using the restrained electrostatic potential (RESP)[38] formalism on the basis of the electrostatic potential evaluated at the same level of theory. A summary of the GAFF atom types and partial charges used to model each additive is reported as Supporting Information (SI, Table S1 and Figure S1). All the DFT calculations were carried out using Gaussian 09.[39]

Simulation Systems Setup. In order to study the face-dependent growth and dissolution dynamics and to estimate the free energy of adsorption through metadynamics, slabs of crystalline urea exposing a single face to the solution were prepared. Initial structures of the {001} and {110} faces were generated from X-ray diffraction data periodically replicated in the 3D space using the software VESTA,[40] thus generating crystalline slabs of the approximate size of 5.5 × 5.5 × 3.0 nm. Each of the two slabs exposing the {001} and {110} faces was embedded in a simulation box of the approximate size of 5.5 × 5.5 × 12 nm, properly filled with water, urea, and additive molecules using the genbox utility included in the GROMACS package.[41] To guarantee a proper representation of both the solid surface and the solution environment and to minimize the impact of simulation artifacts due to the periodic boundary conditions, the size of the volume attributed to the solution was chosen to be at least double than that of the crystalline slab.

MD Simulations. The investigation of the solid/liquid interface dynamics was carried out through standard MD simulations. All the simulations were performed with GROMACS 4.5.3[41] in explicit TIP3P water solvent. A nonbonded cutoff of 1.0 nm was chosen as a compromise between the accuracy of the calculation and the computational effort needed to obtain significant sampling of the growth events in the time scale of tenths of μs. Three-dimensional periodic boundary conditions were applied, treating long-range electrostatic interactions with the particle mesh Ewald approach. The LINCS algorithm was used to constrain the bond lengths enabling the use of a 2 fs time step. Each system was at first minimized with the conjugate gradient algorithm with a tolerance on the maximum force of 300 kJ mol^{-1} nm^{-1}, then a 100 ps NVT equilibration was run to relax the system and to avoid nonphysical contacts between molecules at the boundaries of the simulation box. All the simulations presented in the results part of this work were run as an isothermal−isobaric ensemble at 1 bar and 300 K using the velocity rescale thermostat[42] and the semiisotropic Parrinello−Rahman barostat[43] as implemented in GROMACS 4.5.3. The choice of a semiisotropic pressure control, already exploited in the literature by Piana et al.,[20] allowed a continuous adaptation of the simulation volume through the scaling of the z coordinate and without inducing sudden changes on the (x,y) plane which could destabilize and induce stresses in the crystalline slab. With this protocol we first equilibrate a crystal slab in the presence of pure solvent. This leads to the partial dissolution of the first crystal layer that

becomes visibly rougher when compared to a complete layer. This configuration was then used to generate the initial sample for the concentrated solution study. After 500 ps of temperature and pressure equilibration, the simulations in the presence of the concentrated solution were extended to longer time scales, typically 0.2 μs, with the aim of investigating surface dynamics during urea dissolution and growth in both the presence and absence of additives and for both the {001} and {110} surfaces. The computational time needed to carry out a typical 0.2 μs MD simulation on 16 CentOS 5 Cray cores was 15−20 days. A summary of the standard MD simulations discussed in the paper is reported in Table 2 in the Results section.

Simulation Analysis. In order to analyze the surface dynamics of a crystal slab in contact with a solution, it is necessary to define measures that allow identifying solute molecules as belonging either to the crystalline or to the liquid phase. Discriminating between the liquid- and crystal-like structure of the i^{th} urea molecule on the basis of its trajectory, i.e., the position of all its atoms at each time t requires the development of a quantitative criterion accounting for the concepts of both local density and local order of the molecular surrounding of the urea molecule itself. In this work the measure of the degree of crystallinity $\Gamma_i(t)$ was developed on the basis of the known orientation of the urea molecules in the crystalline structure as the product of two functions, $\rho_i(n_i(t))$ and $\phi_i(n_i(t), \vec{\theta}_i(t))$, which describe the local density and local order, respectively. These functions are defined as

$$\rho_i(n_i(t)) = \begin{cases} \exp\left(-\dfrac{(n_i(t) - \overline{n})^2}{2\sigma_n^2}\right), & n_i(t) \le \overline{n} \\ 1, & n_i(t) > \overline{n} \end{cases} \quad (1)$$

$$\phi_i(n_i(t), \vec{\theta}_i(t)) = \frac{1}{n_i(t)} \sum_{j=1}^{n_i(t)} \left\{ \exp\left(-\frac{(\theta_{i,j}(t) - \overline{\theta}_0)^2}{2\sigma_\theta^2}\right) + \exp\left(-\frac{(\theta_{i,j}(t) - \overline{\theta}_1)^2}{2\sigma_\theta^2}\right) \right\} \quad (2)$$

where $n_i(t)$ is the number of neighbors of the i^{th} urea molecule, i.e., those molecules for which the distance between the carbon atoms of the molecules is less than an arbitrary cutoff, which was taken as 0.6 nm in this work; $\overline{n}$ is the minimum number of neighbors within the same cutoff that are found for a molecule belonging to the exposed surface of the crystalline phase at the interface; σ_n is the standard deviation of the Gaussian distribution of $\overline{n}$ in the solid; $\vec{\theta}_i$ is the vector of the n_i mutual orientations $\theta_{i,j}$ between the internal vectors associated with the i^{th} urea molecule and its j^{th} neighbor. In this work, the internal vector is defined along the carbonyl bond of the urea molecule. Since the molecules in the crystalline solid are not completely still, their orientation with respect to each other fluctuates slightly over time; σ_θ expresses the extent of these fluctuations whereas $\overline{\theta}_0$ and $\overline{\theta}_1$ are the mutual orientations of the internal vector defined in each urea molecule with respect to its neighbors in the crystalline solid. The state of the i^{th} urea molecule then is defined at every time t in terms of degree of crystallinity by

$$\Gamma_i(t) = \rho_i(n_i(t))\varphi_i(\vec{\theta}_i(t)) \quad (3)$$

which assumes values in the [0;1] interval, where the lower end represents a molecule in the liquid phase and the upper end a molecule in the crystal. A summary of the values used in the trajectory postprocessing for the calculation of $\Gamma_i(t)$ is reported in Table 1.

Given the Γ_i values computed for all the urea molecules in the system, the number of molecules belonging to the crystalline phase at each time step t can then be straightforwardly obtained as

$$N_C(t) = \sum_{i=1}^{N_{tot}} \Gamma_i(t) \quad (4)$$

where N_{tot} is the total number of urea molecules in the simulation box. It is worth to highlight that $\Gamma_i(t)$ is a function that describes the crystallinity of each molecule assuming values that are not necessarily integers contrary to, for example, a time correlation or a radial distribution function that describe the crystallinity of an ensemble. This leads to a total number of crystalline molecules in the simulation box computed with eq 4, which is not necessarily an integer. With this approach both the global evolution of the molecular system and the local state of each urea molecule were quantitatively evaluated through $N_C(t)$ and $\Gamma_i(t)$, respectively. The quantitative evolution of the molecular system can be characterized also in terms of the number of molecules in the liquid phase, defined as $N_L(t) = N_{tot} - N_C(t)$ and the variation in the number of molecules in the crystalline state $\Delta N_C(t) = N_C(t) - N_C(t = 0)$.

Table 1. Parameters Used for the Calculation of the Molecule-Based Degree of Crystallinity Γ_i

parameter	value
cutoff	0.6 nm
$\overline{n}$	4
σ_n	1
$\overline{\theta}_0$	0°
$\overline{\theta}_1$	180°
σ_θ	27.5°

In order to quantitatively assess the evolution of the crystalline layers, growing or dissolving at the solid/liquid interface, the system volume was discretized in slices with the thickness given by the characteristic height of the lattice step in the direction orthogonal to the exposed surface. This allows for the calculation of $N_{tot,k}$, the total number of urea molecules in the k^{th} slice by direct count and $N_{C,k}$, the number of crystalline molecules in each of them, as

$$N_{C,k} = \Sigma_{i \subset k^{th}\text{layer}} \Gamma_i(t) \quad (5)$$

Computing the evolution of $N_{C,k}$ allows to follow the growth dynamics of each layer over the course of a simulation. In order to compare MD simulations of the {001} and {110} surfaces, $N_{C,k}$ was normalized by dividing by N_{surf}: the number of molecules contained in a complete crystalline layer; N_{surf} is a face-specific parameter determined by the finite size of the simulated system.

To further characterize the growth dynamics at the solid/liquid interface, two characteristic ratios were computed for each volume slice representing, respectively, the degree of crystallinity and the density of the growing layer:

$$O_k = \frac{N_{C,k}}{N_{tot,k}} \quad (6)$$

$$D_k = \frac{N_{tot,k}}{N_{surf}} \quad (7)$$

Collecting statistics on these two parameters allowed to build bidimensional pseudo free energy surfaces (pseudo-FES) resembling the process of formation or dissolution of a crystalline layer on each considered face. The term pseudo-FES is here used to highlight that the probability distributions in the (O_k, D_k) space are gathered from MD simulations in which the nonequilibrium process of crystal growth is observed under a continuously varying composition in the liquid phase. Therefore the pseudo-FES provide a convenient representation of the pathway followed in the order/density space during the growth of crystal layers rather than providing a quantitative description of the thermodynamics associated with this process. Moreover the pseudo-FES term has been introduced to make a distinction between the aforementioned representations of the sampling obtained by classical MD and the FES obtained with well-tempered metadynamics, later proposed to rigorously discuss the interaction between an additive molecule and the crystal surfaces. Given the probability distribution $p(O_k D_k)$ the pseudo-FES, F, was directly computed using the Kirkwood equation:[44]

$$F(O_k, D_k) = -k_B T \ln p(O_k, D_k) \quad (8)$$

Free Energy Calculations. An estimate of the free energy associated to the adsorption of both urea and additives on a given urea crystal surface was obtained through WT metadynamics,[45,46] a simulation technique aimed at enhancing the sampling of rare events through the application of a history-dependent bias potential to a set of collective variables (CVs). As a complete and exhaustive description of WT metadynamics goes beyond the scope of this paper, we refer the interested reader to the papers introducing metadynamics[45] and WT metadynamics[46] as well as a recent review of their applications in material science, chemistry, and biochemistry.[47] Moreover a brief description of the methods principles and working equations is provided in the SI. In this work the FES associated with the adsorption was calculated through WT metadynamics for each component as a function of two CVs, i.e., the Cartesian position in the direction orthogonal to the crystal surface (hereafter referred to as CV_1) and the molecule orientation, which is described as the angle between an arbitrary internal molecular vector and a vector orthogonal to the crystalline surface (hereafter referred as CV_2). This choice allowed to resolve both the bound and the unbound states in the (CV_1,CV_2) space as well as differently oriented bound configurations. In order to speed up the exploration of the simulation box, a constrain potential has been applied to a specific atom of the foreign molecule in a way similar to what was suggested by Roux et al.[48,49] The free energy calculations were performed with GROMACS 4.5.3 equipped with the PLUMED[50] plugin.

RESULTS AND DISCUSSION

Combining MD and metadynamics simulations allows us to highlight several molecular details of the growth and inhibition mechanisms of urea crystal growth from water solution. To this end, the simulations reported in Table 2 are analyzed. In these simulations the driving force for a net growth of the crystalline phase is the supersaturation of the liquid phase. We found that in the finite-sized volume confined between two urea surfaces, the urea equilibrium concentration is between 3 and 4 mol/L, in agreement with results of simulations reported in the literature.[19] To induce crystal growth, the initial concentration of the liquid phase was set to values >7 mol/L.

Table 2. Summary of the Standard MD Simulations Discussed in the Results Section

label	face {*hkl*}	initial urea conc (mol/L)	simulation time (μs)	additive	additive conc (mol/L)	additive/ surface mol. ratio
A	{001}	7.25	0.2	–	–	–
B	{110}	7.40	0.2	–	–	–
C	{001}	7.25	0.2	biuret	0.62	0.18
D	{001}	7.25	0.2	biuret	1.08	0.33
E	{001}	7.25	0.2	acetone	0.62	0.18
F	{001}	7.25	0.2	acetone	1.08	0.33
C′	{001}	8.5	0.2	biuret	0.62	0.18
D′	{001}	9.0	0.2	biuret	1.08	0.33
E′	{001}	7.0	0.05	acetone	0.62	0.18
F′	{001}	7.3	0.05	acetone	1.08	0.33
G	{110}	7.4	0.2	biuret	0.13	0.08
H	{110}	7.4	0.2	biuret	0.26	0.16
I	{110}	7.4	0.2	acetone	0.13	0.08
J	{110}	7.4	0.2	acetone	0.26	0.16

In order to investigate the effect of additive molecules on crystal growth, two additives were investigated: acetone and biuret; their concentrations were set such that the behavior of the molecules on each crystal face could be determined and that crystal growth was not completely inhibited. The differences in the additive concentrations from the simulations of the {001} (C–F in Table 2) and the {110} (G–J in Table 2) faces are due to the intrinsically different growth mechanisms that determine a different sensitivity to the finite size of the implemented molecular model, as will be discussed in the following.

The results have been analyzed in order to describe both the growth and the inhibition mechanisms with a hierarchical approach, i.e., by defining appropriate quantities on the scale of the whole simulation, then on the scale of single crystalline layers, and finally on the scale of a single urea molecule using the methodology and quantities presented in the Methods section.

Growth Mechanisms. The standard MD simulations of the {001} and {110} faces uncovered, with atomistic detail, the intrinsic mechanisms that govern crystal growth on the fast and slow growing face, respectively. In the following paragraphs the results obtained from simulations A and B (Table 2) are discussed focusing on the evolution of the whole model and the crystal layer. The discussion regarding the scale of the single urea molecule is reported in the SI.

Scale of the Crystal. Performing standard MD simulations, a net growth of the crystalline phase was observed for both the {001} and the {110} faces over a time span of the hundreds of nanoseconds. The evolution of the whole simulated crystal is illustrated in Figure 1a where the increase in the number of crystalline–solid molecules, ΔN_C, on both faces is shown, together with the evolution of the number of molecules in the liquid phase, N_L. The decrease in time of N_L means that the driving force of crystallization, i.e., the supersaturation, progressively decreases over the course of the simulation, which is caused by the fact that the simulations are performed at constant number of molecules, hence the liquid phase is inevitably depleted as the crystal grows. It can immediately be seen that the evolution of $\Delta N_C(t)$ exhibits two remarkably different trends for the {001} and {110} faces. The profile for the fast {001} face consists of a rather smooth curve that gradually flattens, i.e., the growth rate of the solid phase decreases as the liquid phase is depleted of urea molecules. For the slow {110} face on the other hand, the growth profile proceeds through two clearly noticeable steps, the first occurring in the first 0.03 μs of simulation and a second at 0.10 μs; between these steps the number of crystalline–solid molecules remains constant. We interpret these different behaviors as the fingerprint of two different crystal growth mechanisms that occur on the different faces, i.e., a continuous, or "rough", growth mechanism for the fast {001} face and a "birth and spread" mechanism for the slow {110} face. In Figure 1b three snapshots of the molecules in the simulation domain, i.e., including crystal and solution, are shown. In these snapshots only the urea molecules present in the simulation box are drawn, while the water molecules, though explicitly present in the simulation, are not shown for the sake of clarity. The urea molecules are depicted as spheres centered on the carbon atom, which are colored according to their degree of crystallinity Γ_i, as defined in eq 3 of the Methods section. This representation allows to interpret the quantitative trends seen in Figure 1a at the molecular scale. It can be observed that, going through the three snapshots, the number of liquid molecules (red) decreases, while the number of molecules in the crystalline solid (blue) grows. Moreover it can be noted that while the majority of the urea molecules depicted in the three snapshots of Figure 1b is in the crystalline ($\Gamma_i = 1$, blue spheres) or in the liquid ($\Gamma_i = 0$, red spheres) state, a minor fraction of molecules is characterized by a semicrystalline state, i.e., by an intermediate

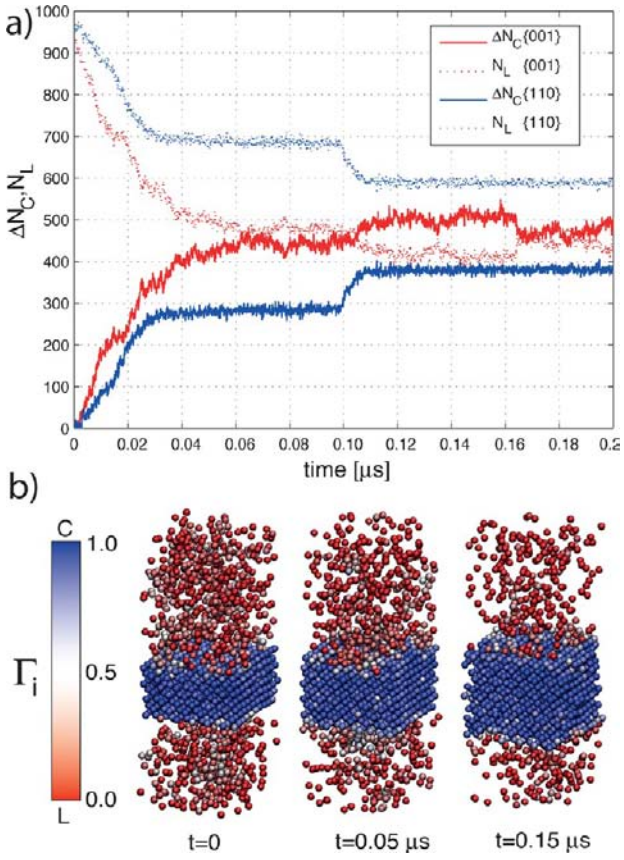

Figure 1. MD simulations of {001} and {110} faces in water (A and B in Table 2). (a) Evolution of the urea molecules included the crystal (solid lines) and of the number of urea molecules in solution (dashed lines) during the A (red) and B (blue) simulations. In both simulations, while the crystal grows, the solution is depleted leading to a stationary state where no net growth is observed. A continuous (simulation A) and a stepwise (simulation B) profile is, respectively, observed for the {001} and the {110} faces. (b) Snapshots from the simulation B at different timesteps. For the sake of clarity water molecules are omitted, while urea molecules are depicted as spheres centered on the carbon atom and colored in function of their degree of crystallinity Γ_i (defined in eq 3).

value of Γ_i. The majority of these semicrystalline molecules is located on the crystal surface, representing the urea molecules interacting with the crystal lattice. A small fraction of the semicrystalline molecules is instead located either in solution, i.e., corresponding to short-lived partially ordered clusters of urea molecules, or in the crystal, i.e., representing random fluctuations of the crystalline molecules.

Scale of the Crystal Layer. The differences in the growth mechanisms appear more clearly when the formation of single crystalline layers growing at the solid/liquid interface is analyzed. The dynamics of the growing layers in contact with the solution over a simulation time span of 0.2 μs for both the {001} and the {110} faces are reported in Figure 2. Focusing on the {001} face, the first two layers (Figure 2, a and a′, note that the prime indicates a crystal layer on the lower crystal face) are readily completed in the presence of the initially concentrated solution. The second layers (b and b′) start to grow almost immediately, although layer b′ takes longer to be fully formed. The formation of the third layer is more sluggish, reaching a steady state in which the crystal is in a dynamical equilibrium with a 4.5 mol/L urea solution (see also Figure 1). At this point of the simulation the supersaturation has decreased to such a low level that no more crystal growth is observed. The slow {110} face on the other hand exhibits sudden growth events on adjacent layers, producing almost complete crystalline layers with rates that look largely independent of the supersaturation. Moreover the growth on multiple layers at the same time does not occur; the newly born crystalline layers spread one at a time to cover the whole model surface.

This dynamic behavior of the growing crystal layers looks again like the fingerprint of two well-known growth mechanisms. On the fast {001} face the addition of urea molecules follows a continuous growth mechanism in which the net increase of crystalline molecules is obtained by independent addition events, whereby each molecule reaching the interface is easily incorporated into the lattice. On the other hand the growth of layers on top of the slow {110} face proceeds with a mechanism, in which urea molecules that are adsorbed on the growing surface, but are not yet incorporated into the lattice, suddenly assemble and are simultaneously incorporated in the crystal. This behavior can be interpreted as a birth and spread mechanism[51] in which the rate-determining step consists of the formation of a stable two-dimensional crystalline nucleus on top of the growing surface.

To further characterize the differences in the growth processes on the two faces, pseudo-FES (see the Simulation Analysis section) were constructed using the Kirkwood relation (eq 8) from the probability distribution collected in the space defined by two parameters, O_k and D_k, as defined in eqs 6 and 7. These two parameters represent the degree of crystalline order and the density of the k^{th} crystal layer. In the (O_k,D_k) space the growth of a layer can be pictured as a trajectory that connects the region around (0,0), corresponding to a new forming layer, with the region around (1,1), corresponding to a completed crystalline layer. The pseudo-FES associated with the layer growth on the {001} and the {110} faces are shown in Figure 3 in k_BT units, where k_B is the Boltzmann constant, as $F = -\ln p(O_k,D_k)$. In this representation the lower the probability $p(O_k,D_k)$, the higher the corresponding F value. The presence of barriers in F higher than k_BT, represents regions in the (O_k,D_k) space where few layer states were found during the simulations, thus indicating that these configurations are not favored.

From the 2D pseudo-FES and their projections on the O_k coordinate (Figure 3), it is seen that on the fast {001} face, the growth of ordered layers proceeds without overcoming energy barriers significantly higher than k_BT. The simulation of the crystal growth on the fast {001} crystal face, in fact, exhibits a rather homogeneous sampling of the (O_k,D_k) space, thus highlighting the accessibility of a continuum of order/density values characterizing the state of growing layers. This interpretation is compatible with a continuous growth mechanism, which proceeds via the independent addition of single molecules to the crystalline lattice. Thereby the increase in density and order of a growing crystal layer occurs at the same time through a process that gradually produces a complete new crystal layer. This feature is well represented by the shape of the pseudo-FES built for the {001} face that corresponds to a smooth trajectory in the density/order space that comprises also regions characterized by low density and relatively high degree of crystallinity, i.e., the dark-blue areas are along the diagonal ($O_k = D_k$) in the (O_k,D_k) plane of Figure 3.

The pseudo-FES relative to the slow {110} face exhibit a different shape, characterized by the presence of two well-defined minima. A first basin (i.e., the region around the minima in the pseudo-FES), located at a low degree of crystallinity, belongs to

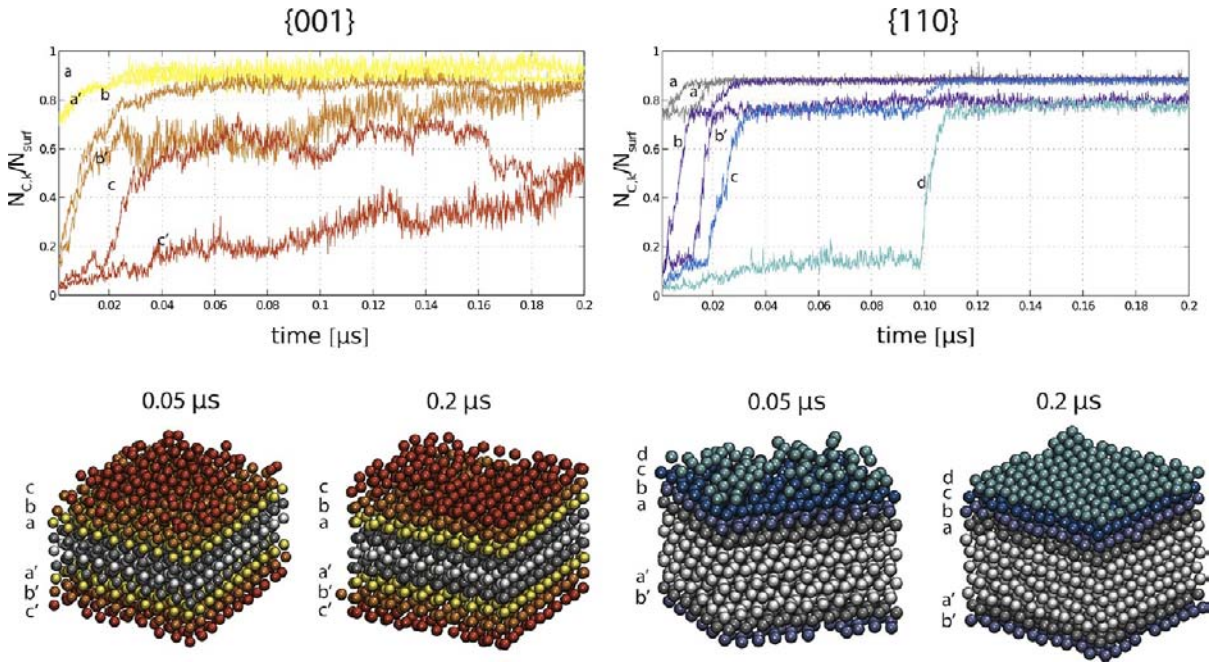

Figure 2. MD simulations of {001} and {110} faces in water (A and B in Table 2). Time series of the normalized number of crystalline molecules in the growing layers $N_{C,k}/N_{surf}$ (refer to the Methods section). Snapshots of the surfaces at 0.05 and 0.2 μs are below each plot. The configurations at 0.2 μs offer a qualitative description of the crystal surface morphology obtained at the end of the A and B MD simulations. The {001} surface is characterized by higher roughness, as several crystalline planes are simultaneously in contact with the solution on both sides of the simulated slab. The {110} face exhibits instead a single almost complete crystalline plane in contact with the solution on each side.

layer configurations in which only a minor fraction of molecules in contact with the surface is included in the crystal lattice, whereas the majority of them are randomly ordered. A second basin can instead be seen for values of degrees of order and density close to one. This basin represents a layer of molecules that are ordered and packed as in the crystal lattice. The two basins are separated by a scarcely populated intermediate region, crossed during the sudden growth events shown as steep steps in Figure 2b. This feature reflects the presence of a significant energy barrier on the pathway toward the growth of a complete crystalline layer. This representation is in agreement with the interpretation of the growth mechanism of the {110} face as a birth and spread process. The birth of a crystalline nucleus that spreads and covers the whole surface on the {110} face is in fact an activated process in which the system needs to overcome energy barriers significantly higher than its thermal noise.

The two-stage process leading to the formation of a complete crystalline layer at the solid/liquid interface exposing the {110} crystal face is also reflected by the shape of the pseudo-FES in the (O_k,D_k) plane. The bimodal character of the shape highlights that the random adsorption of urea molecules and their inclusion in the growing crystal are two distinct phenomena. Moreover the pseudo-FES describes a path above the diagonal $(O_k = D_k)$ in the (O_k,D_k) plane. This means that the spread of the critical embryo starts from a relatively dense layer of adsorbed molecules and evolves through the diffusion and reorientation of urea molecules already adsorbed on the surface. Both phenomena are independent from the concentration in solution and explain the constant shape of the curves represented in Figure 2b.

From this picture it emerges that the growth on the fast and slow faces is inherently governed by different phenomena. The rate of molecule addition to the crystal lattice on the fast {001} face depends in fact on the rate with which urea molecules get in contact with the surface, and it is therefore dependent on the urea concentration in the liquid phase. The rate-determining step of the crystal growth process on this face is the diffusion of urea molecules toward the surface. The rate-determining step of the slow {110} face growth is instead the nucleation of a stable crystalline two-dimensional nucleus on the surface. The global growth rate of this face is therefore determined by the frequency of nucleation events at the solid liquid interface. It is inherently clear that this phenomenon has a stochastic character, so that calculating a quantitative growth rate for the slow {110} face is not feasible.

This picture is consistent with the molecular morphology exhibited by the {001} and the {110} faces and sketched in the insets in Figure 3. In fact, solid/liquid interfaces exposing the fast {001} face exhibit a high density of hydrogen-bond donors and acceptors, as the {001} plane is orthogonal to the periodic hydrogen bond chain responsible for a large part of the cohesion of the crystalline solid. On this face molecules are naturally oriented in such a way to establish crystal-like hydrogen bonds with the urea molecules approaching the surface. On the slow {110} face, on the contrary, the moieties capable of establishing hydrogen bonds are oriented orthogonally with respect to the exposed surface, therefore the direct inclusion in the crystal lattice of single urea molecules is unlikely. However once a crystalline bidimensional nucleus is formed on the {110} face, the spreading process occur once again in a direction parallel to the aforementioned periodic hydrogen-bond chain.

This interpretation of the growth mechanisms based on molecular details uncovered by MD simulation is in good agreement with the classical description of birth and spread and continuous growth mechanisms as well as with the body of knowledge regarding urea crystallization in water. Although, the mechanistic detail gives a valuable insight on the pathway followed by crystal growth on morphologically different surfaces, a quantitative assessment of the growth rates remains heavily

dx.doi.org/10.1021/ja307408x | J. Am. Chem. Soc. 2012, 134, 17221−17233

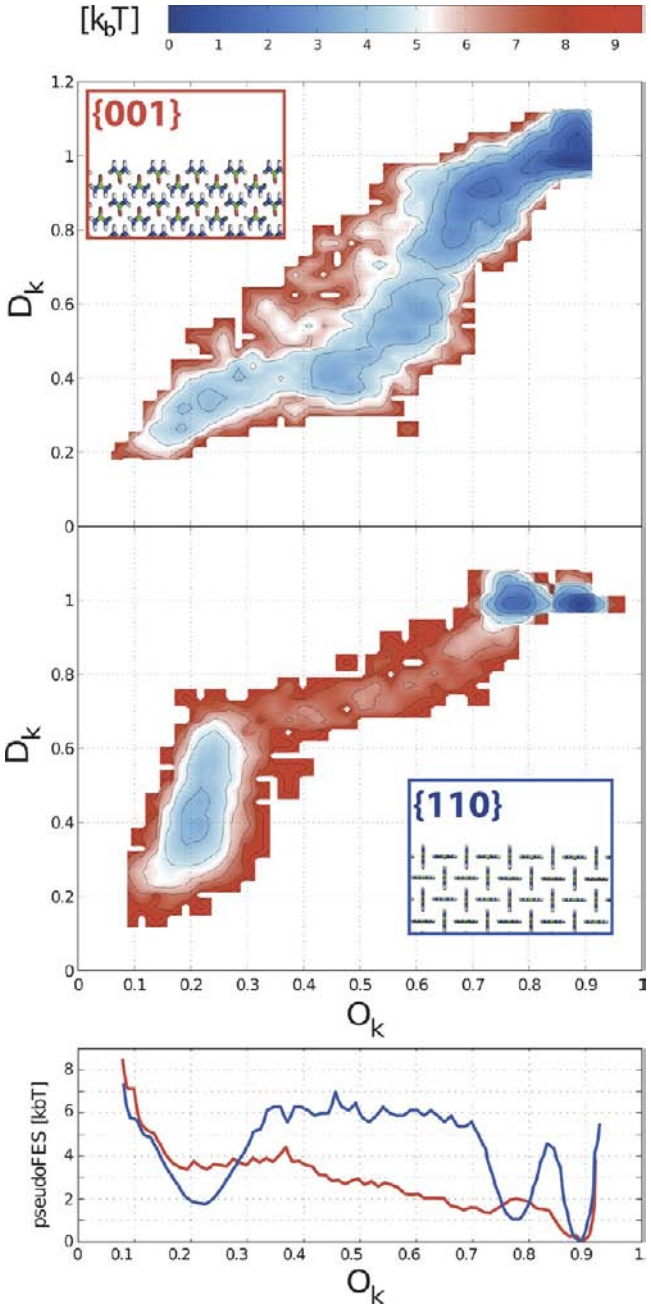

Figure 3. MD simulations of {001} and {110} faces in water (A and B in Table 2). Pseudo-FES in the space defined by O_k and D_k, respectively, resembling degree of crystalline order and the density of the crystalline layers on the {001} face (upper panel) and the {110} face (lower panel). In the insets are reported the molecular morphologies exhibited by the {001} and the {110} faces. The projection of the FES on the O_k highlights the remarkable differences observed in the growth mechanisms. While on the {001} surface the formation of a crystalline layer occurs without any significant energy barrier, and on the {110} face an energy barrier of $\sim 4k_BT$ separates a disorderedly adsorbed layer from a fully crystalline one.

affected by the finite size of the simulation box. On the {110} face the critical size of crystalline nuclei is underestimated due to the artificial stabilization caused by the periodic boundary conditions of the simulation box. This manifests itself in an overestimation of the frequency of birth of stable nuclei on the {110} face and therefore of the global growth rate of the crystal. The size dependence of the urea growth rate on the {110} face was investigated by comparing the ΔN_C trends in two molecular models of different size. More information on this effect can be found in the SI.

While on the one hand this finite size effect hinders the possibility to directly compare results from MD simulations to experimental observations, on the other hand it allows to explicitly observe the concerted molecular mechanism which determines the growth on the {110} face. Monte Carlo simulations and experiments[19,20] show that, in water, growth on the {110} face occurs at a very slow rate. This is in qualitative agreement with our findings: the frequency of birth and spread events becomes in fact the lower the closer we get to simulating an infinite nonperiodic slab. Since on the fast-growing face {001} the rate-determining step for crystal growth is the diffusion of urea molecules toward the growing surface, the stabilization of crystalline islands, which is an artifact of the periodic boundary conditions, does not affect the observed growth rate.

Effect of the Additives. The insight into the dynamics of crystal growth achieved through MD simulations provides the background against which the molecular effect of additives can be assessed. Here we have studied the effects of the additives biuret and acetone on the growth of the {001} and {110} faces. We contrast biuret with acetone, since it has a lower structural compatibility with the urea lattice while having comparable size and sterical hindrance. To understand the effect of the additives on the growth mechanism, the evolution of the total number of crystalline molecules and the evolution of individual crystal layers were extracted from MD trajectories. The effect of the additive on the crystal growth mechanism has been investigated with two series of simulations, performed starting from an equilibrated crystal surface exposing the {001} or the {110} crystal face to a liquid phase consisting of solute solvent and additive; details of the simulations conditions are reported in Table 2. As the characteristic time for the equilibration of the urea molecules between the crystalline and the liquid phase in the molecular models of the {001} surface is comparable with that of the formation of an equilibrated adsorbed layer of additive on the surface, the simulations of the {001} face were divided in two parts: A first production phase performed starting from a clean urea surface (simulations C−F, Table 2) allowed the study of the two phenomena simultaneously occurring on the surface. A second stage (simulations C′−F′, Table 2) was then carried out starting from the final configuration of the crystal obtained at the end of the first stage. This configuration exhibits a crystal surface covered by an equilibrated layer of adsorbed additive molecules. This second stage allowed to further highlight the reduction of the growth rate due to different additives. This study has then been complemented with the description of the adsorption thermodynamics of a single additive molecule on both the fast {001} and the slow {110} growing faces.

Scale of the Crystal. The evolution of the crystal surfaces has been studied in the presence of biuret and acetone at different concentrations. The increase in the number of the crystalline solid molecules ΔN_C for both {001} and {110} faces in the presence of acetone and biuret is shown in Figure 4. Note that also in this case while the growth rate on the fast {001} face does not depend on the finite size of the model surface, the growth rate on the slow {110} face is instead enhanced by the finite size of the model that produces an increased stabilization of the crystalline embryos on the surface due to the periodic boundary conditions. Moreover, the simulations are again carried out keeping the total number of molecules in the simulation volume constant, therefore the liquid phase is depleted of urea molecules as the

dx.doi.org/10.1021/ja307408x | J. Am. Chem. Soc. 2012, 134, 17221−17233

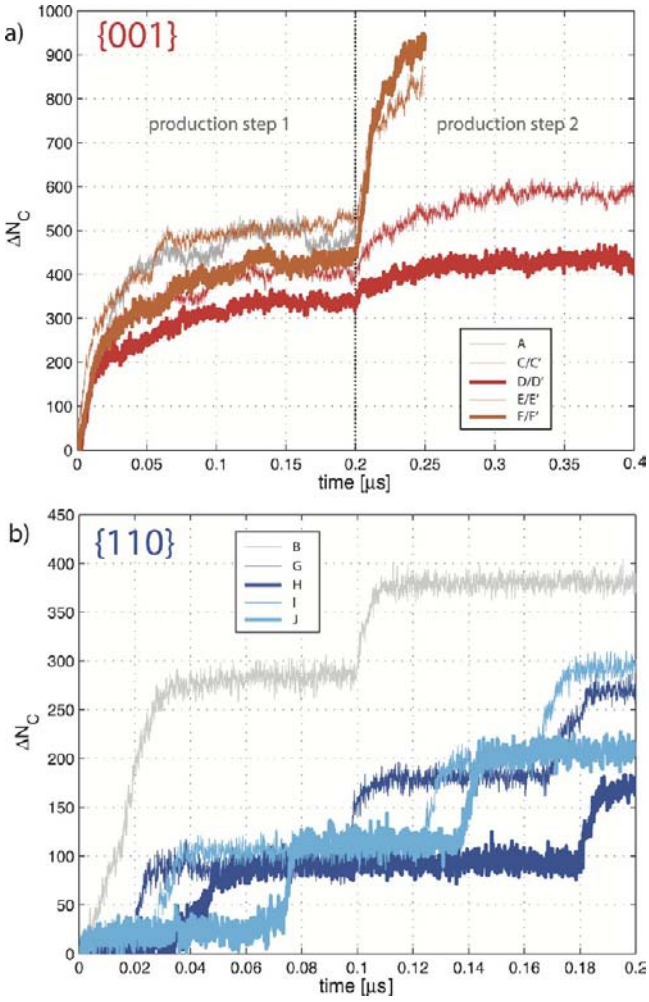

Figure 4. MD simulations of urea growth in presence of biuret and acetone. Evolution of the number of molecules included in the crystal lattice ΔN_C for the {001} (a) and {110} (b) faces. The labels reported in both figures refer to Table 2.

crystal grows. These aspects make a quantitative determination of growth rates and a direct comparison of the results obtained for the {110} and the {001} faces problematic. Nevertheless the shape of the ΔN_C reflects the growth mechanism occurring at the molecular level. The curves showing the evolution of ΔN_C for the {001} face maintain the same shape observed in the absence of additives. The curves showing the evolution of the {110} models exhibit again the stepwise shape observed without additives. From the curves reported in this figure, it can be observed that the presence of additives affects the net growth of the crystal on both faces. Focusing on the growth of the {001} face (Figure 4a), two aspects clearly emerge: In the first production phase, when the additive and the solute molecules compete for the interaction with the {001} face, the total number of molecules included in the crystal decreases with the increase of the additive concentration. Moreover the effect is significantly dependent on the chemical nature of the additive. While biuret induces a remarkable reduction of the growth, acetone shows a barely observable effect. This effect emerges even more clearly in the second production phase. The addition of urea molecules on a {001} face equilibrated in the presence of additive molecules is in fact evidently slowed down when biuret is present while appears to be close to that of a pure urea system in the case of acetone. Likewise, the curves belonging to the {110} face can be interpreted as indicating that the presence of both biuret and acetone hinders the growth of this face to roughly the same extent. The slow down however correlates neither with the chemical nature nor the concentration of the additives, thus suggesting a generic sterical hindrance rather than the establishment of specific interactions with the {110} face.

Scale of the Crystal Layer. To further characterize the growth mechanisms in the presence of additives, the dynamics of formation of individual crystalline layers has been analyzed. The effect of additives on the growth of single crystalline layers can be seen in Figure 5, which has to be contrasted with the case of pure urea, reported in Figure 2. In Figure 5 one can see that the layers on the {001} face (simulations C−F) are less crystalline (i.e., they have a lower $N_{C,k}/N_{surf}$ ratio) than the corresponding layers growing in the pure urea case at similar times, while the lower layers do not reach full completion during the time of the simulation.

This effect is more pronounced for biuret than for acetone (simulations C vs E and D vs F) and becomes more visible when the additive concentration is increased (simulations C vs D and E vs F). This behavior is caused by the additive molecules adsorbing on the crystal face and competing with urea for surface interaction sites; biuret exhibits a higher effectiveness in that than acetone. As the incorporation of urea molecules into the crystal occurs one molecule at a time in the direction orthogonal to the surface, additive molecules adsorbed on the {001} face reduce the growth by reducing the accessibility of surface lattice sites.

On the {110} surface on the other hand (simulations G−J), the most evident feature in the evolution of the layers is the reduction in the frequency of birth and spread events, whereas the formed layers appear to be as complete as in the pure case. This phenomenon can be interpreted as an increase in the induction time for the bidimensional nucleation phenomenon occurring on this surface. The additive reduces in fact the probability of forming a stable bidimensional crystalline embryo, which determines the stochastic nature of the birth and spread mechanism responsible for the growth on the {110} face. This is confirmed by the fact that the spread phase (identifiable with the noticeable steps in Figures 2 and 5), occurring in the direction parallel to the crystal surface, is marginally affected by the presence of additives. The fact that sterical hindrance is the key aspect of the growth reduction on the {110} urea face is confirmed by the fact that no major difference is observed between biuret and acetone. This indicates that on the {110} face, additives are nonspecifically adsorbed rather than specifically blocking growth sites by fitting into the crystal lattice.

Scale of the Single Additive Molecule. The specificity of the crystal-face/additive interaction emerges as a key factor for the understanding of the inhibition mechanism and will be elucidated in the following. Figure 6a illustrates the distribution of the orientations of the additive molecule with respect to the {001} surface for biuret and acetone, here expressed as the angle formed by an internal vector defined for each single molecule and the direction orthogonal to the crystal surface (illustrated in Figure 7a). Biuret exhibits two marked maxima which correspond to specific oriented configurations, whereas acetone on the contrary does not display any remarkable orientation preference. In Figure 6b the number of adsorbed additive molecules over time is plotted. It can be seen that more biuret molecules are adsorbed (at similar additive concentrations) than acetone and that the number of adsorbed molecules approaches a plateau already after about 20 ns, which indicates a stronger

dx.doi.org/10.1021/ja307408x | J. Am. Chem. Soc. 2012, 134, 17221−17233

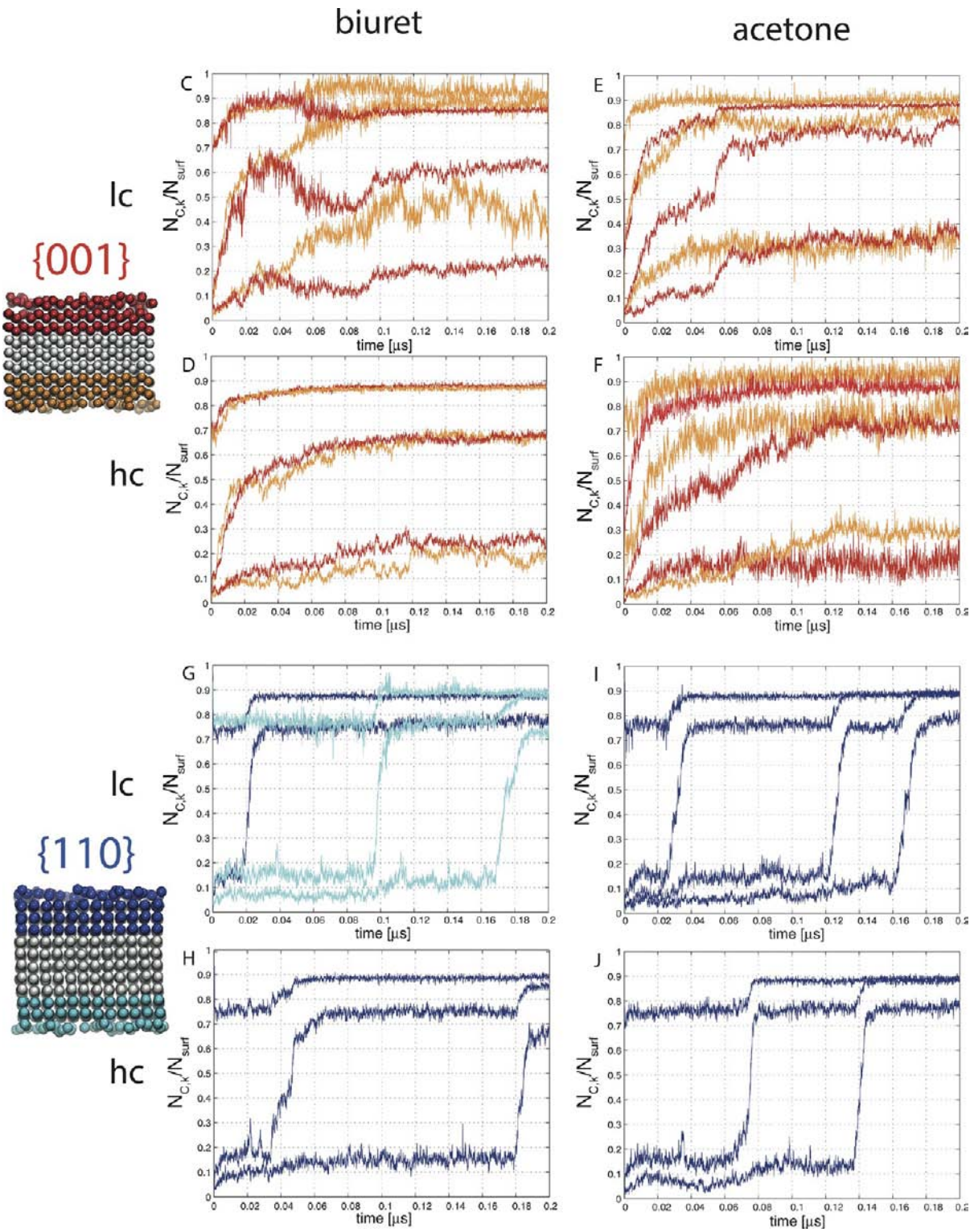

Figure 5. MD simulations of {001} and {110} faces in the presence of additives. Time series of the normalized number of crystalline molecules in the growing layers $N_{C,k}/N_{surf}$ (see the Methods section) obtained from the 0.20 μs simulation of {001} and {110} urea crystal faces in contact with biuret and acetone at different additive concentrations. The subfigures are labeled according to Table 2. It can be observed that the presence of additives causes two differents effects on the different faces. On the {001} face, especially in the case of biuret, it causes the reduction of the number of crystal-like molecules included in the growing layers. On the {110} face, both biuret and acetone reduce the frequency of the birth and spread events, without changing the completeness of the produced crystal layers.

interaction of biuret with urea compared to the one of acetone with urea. Figure 6a,b demonstrates that the interaction between biuret and urea is both stronger (number of molecules adsorbed) and more specific (specific orientations) than the interaction between acetone and urea. The strength and specificity are caused by the structural complementarity between the functional groups present in the additive molecule and the functional groups of urea present at the {001} face. In fact, this proves to be

dx.doi.org/10.1021/ja307408x | J. Am. Chem. Soc. 2012, 134, 17221−17233

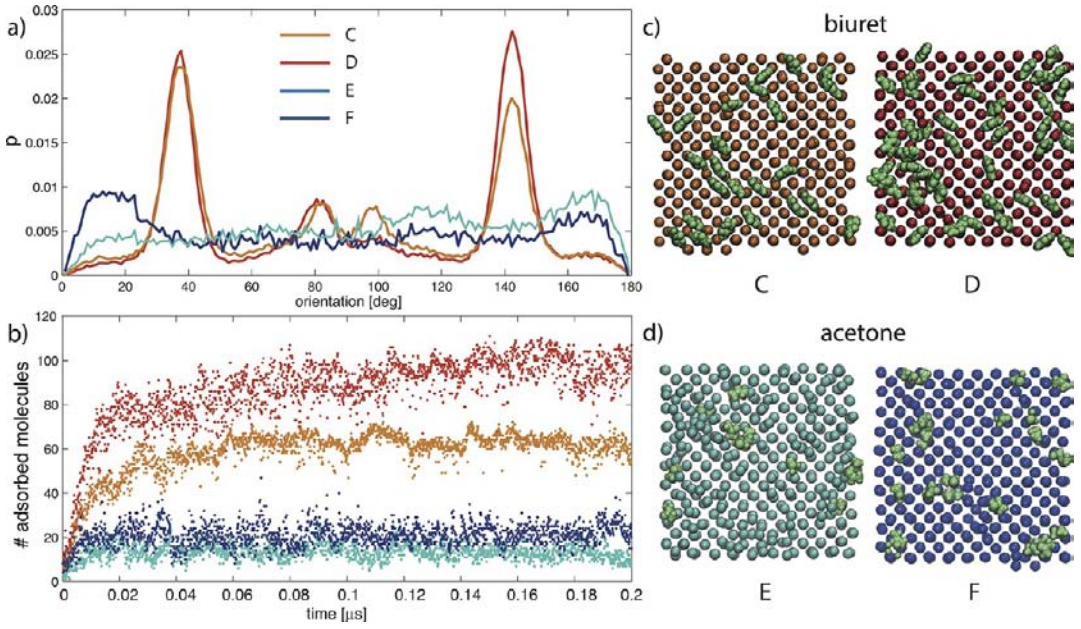

Figure 6. MD simulations of {001} faces in the presence of additives. (a) Probability distribution of adsorbed additives orientation expressed as the angle between a properly defined molecular vector and the vector orthogonal to the crystal surface. The probabilities were calculated from the unbiased MD simulations on the {001} face for biuret and acetone. The molecular vector was defined as parallel to the C═O bond in the acetone molecule and as parallel to the axis connecting the two carbon atoms C and C1 (see Figure 7a) in the biuret molecule. (b) Number of biuret and acetone molecules adsorbed during the simulation time span on both the top and the bottom surfaces of the simulated crystal slab. Top views of the {001} face with adsorbed (c) biuret and (d) acetone, respectively. The data shown have been extracted from simulations C and D for biuret and E and F for acetone. Urea molecules are represented as spheres centered on the carbon atom, while additive molecules are depicted with atomistic detail using green vdW spheres (biuret 12 green spheres in (c) acetone 10 green spheres in (d)).

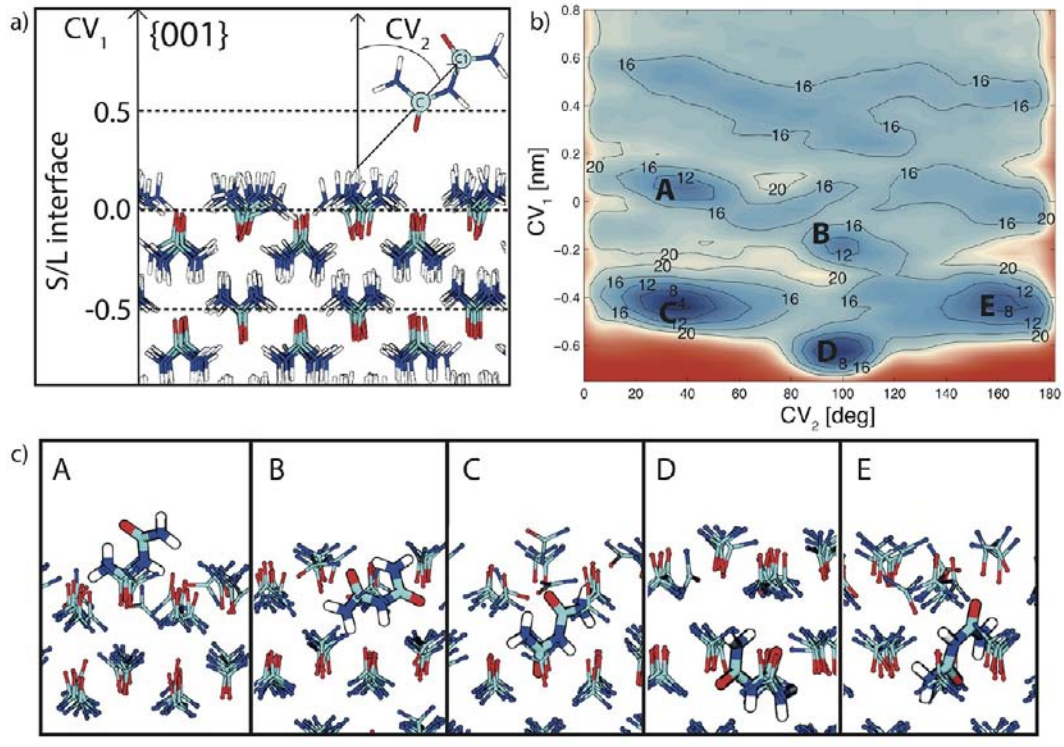

Figure 7. WT metadynamics simulation the adsorption of a single biuret molecule on the {001} face. (a) Graphical legend for the definition of CV_1 and CV_2. (b) FES obtained for biuret as a function of CV_1 and CV_2 relative to the {001} face, the isoenergy values are reported in k_BT. (c) Stable molecular configurations corresponding to the minima of the FES, labeled from A to E according to their correspondent minimum in (b). Structures A, C, and E are characterized by an orthogonal orientation with respect to the crystal face. Structures B and D are instead parallel to the crystal face.

dx.doi.org/10.1021/ja307408x | J. Am. Chem. Soc. 2012, 134, 17221−17233

a key ingredient in the occurrence of surface-selective growth inhibition in the case of urea. It is however worth noticing that despite the strong and specific interaction and the similarity between the two molecules, we never observed any inclusion event of biuret molecules in the urea lattice. The additive merely adsorbs on the crystal face for some time during the simulation and reversibly attaches and detaches from the urea crystal lattice sites exposed to the solution.

The molecular details of the additive/surface interactions were further investigated by means of WT metadynamics simulations in which single additive molecules were driven to explore the (CV_1,CV_2) space, as defined in the Methods section. Here we focus on the interaction of biuret with the fast growing {001} face.

In Figure 7 the FES describing the adsorption of a single biuret molecule on the {001} urea face is reported. The FES represents the detail of the configurations adsorbed on the urea crystal surface, i.e., those located within 0.5 nm of the solid/liquid interface. Representative structures of the states defined by the minima of the FES in the $(CV_1,CV_2$ space) are also reported in Figure 7. Three low-energy regions can be identified: The first region is characterized by $0 < CV_2 < 60$, the second by $60 < CV_2 < 120$, and the third by $120 < CV_2 < 180$. These regions correspond to configurations in which the biuret is parallel, orthogonal, and antiparallel, with respect to an axis perpendicular to the crystal surface, respectively. Moreover the {001} surface is dynamically in equilibrium with the solution through the addition and dissolution of single urea molecules. The interaction of the additive with the crystal at the S/L interface can occur in the first or second crystal layers. However no additive molecule was ever covered by an additional layer of urea molecules, i.e., no biuret molecule was ever permanently built into the crystal. The presence of several well-defined minima describing interacting configurations between the crystal and the additive highlights the fact that well-defined interactions are responsible for the adsorption of biuret molecules on surface sites on the {001} surface. The minimum energy structures found can be grouped in two subsets considering their orientation with respect to the crystal surface. Parallel structures (B and D, Figure 7b) resembling the expected configuration published by Davey and co-workers[16] and orthogonal structures (A, C, and E, Figure 7). From our free energy calculations the orthogonal structures are slightly favored energetically; in both cases however the additive molecule takes advantage of the structural complementarity with the crystal structure, and a dynamical equilibrium between these structures is observed during both enhanced sampling and standard MD simulations.

These features were not found for biuret molecules adsorbed on the {110} face. Here the main preferential orientation represents biuret molecules randomly flattened on the crystal surface, and no specific interactions with the crystal sites were observed in this case. For acetone no strong specific orientation preferences were observed. Similarly to the approaches based on the calculation of the attachment energy,[52−54] the anisotropic crystal growth of urea was further characterized through the calculation of free energies of adsorption of single additive and urea molecules both on the {001} and the {110} face. WT metadynamics allows in fact to readily compute the free energy associated to the adsorption events and therefore to account explicitly for the presence of the solvent and for the entropic effects. Given the free energies of adsorption of a given additive on the {001} and {110} surfaces, we define the parameter surface selectivity $S_{\{001\},\{110\}}$ as the ratio between the adsorption equilibrium constants calculated as

$$S_{\{001\},\{110\}} = \frac{K^{ads}_{\{001\}}}{K^{ads}_{\{110\}}} = \exp\left(-\frac{\Delta G_{ads,\{001\}} - \Delta G_{ads,\{110\}}}{RT}\right) \quad (9)$$

The surface selectivity allows to quantify the preferential interaction of a given molecule, solute or inhibitor, between two specific crystal faces. The adsorption free energies and the values of the $S_{\{001\},\{110\}}$ calculated for acetone, biuret, and urea are reported in Table 3.

Table 3. Adsorption Free Energies and $S_{\{001\},\{110\}}$ Calculated for Acetone, Biuret, and Urea[a]

molecule	$\Delta G_{ads,\{001\}}$ [kcal/mol]	$\Delta G_{ads,\{110\}}$ [kcal/mol]	$S_{\{001\},\{110\}}$
acetone	−0.66 ± 0.38	−1.47 ± 0.45	0.26
biuret	−4.55 ± 1.02	−2.48 ± 0.43	32.81
urea	−3.22 ± 0,83	−1.7 ± 0.39	12.98

[a]The ΔG was computed as a time-weighted average as in the work of Berteotti et al.[55] The error reported is the standard deviation of the time-weighted average. The time-dependent realizations of the ΔG are reported in the SI.

With the calulation of two lumped parameters, such as the affinity for the fast face $\Delta G_{ads,\{001\}}$ and the face selectivity $S_{\{001\},\{110\}}$, made practically achievable by the use of enhanced sampling techniques, we could capture and rationalize the effect of the additives observed during standard MD simulations. In particular the values of ΔG_{ads} and $S_{\{001\},\{110\}}$ show that the interaction of the biuret molecule with the urea crystal faces is much stronger than that of the acetone molecule and also that the selectivity of the biuret for the fast {001} face is remarkable. This evidence allows us to demonstrate the selective adsorption of biuret molecules on the {001} faces of the urea crystal and thus to rationalize why biuret is such an excellent growth inhibitor for these faces; biuret has a higher probability to interact with the fast face than with the slow one and at the same time has a free energy of adsorption comparable to urea itself on the same face. These two properties are caused by the capability of biuret to fill a lattice site on the {001} faces nearly perfectly and can be indeed identified as responsible for the remarkable influence of biuret on the shape of urea crystals.

CONCLUSIONS

In this work we demonstrate the molecular mechanism underlying the effect of additives on the growth of urea crystals in water. At first we have investigated with extensive standard MD simulations the growth of the {001} and the {110} crystal faces. We have identified two intrinsically different growth mechanisms: the {001} face grows following a rough growth process, while the {110} face grows through a birth and spread mechanism, a two-step process characterized by the nucleation of crystalline embryos on the surface and their subsequent enlargement. These mechanisms are consistent with the molecular structure exhibited by the two faces. The {001} face is characterized by the exposure of hydrogen bonds oriented in the growth direction, a feature that favors the direct incorporation in the crystal lattice of urea molecules adsorbed on the surface. The main periodic hydrogen-bond chains are instead parallel to the {110} face, which does not offer sites

capable of easily binding urea molecules in a crystal-like configuration. Due to this feature the growth of new layers occurs through a concerted mechanism involving first a small cluster of 10−20 urea molecules that produces a stable nucleus and then rapidly spreads. The spread of the nucleus proceeds through the addition of urea molecules at the kink sites present at the nucleus edges. This process is extremely fast compared to the nucleation stage as it occurs in the direction of the main hydrogen-bond chain which favors the direct incorporation of urea molecules in the crystal.

We have then analyzed the growth in the presence of additives, such as biuret and acetone. We have found that biuret has a remarkable structural compatibility with the urea lattice sites exposed on the {001} face. It is adsorbed on the {001} face in specific orientations due to the formation of hydrogen bonds with the exposed lattice sites. When adsorbed on the {110} face biuret shows instead a lower compatibility with the crystalline lattice. This leads to the remarkable selectivity of the biuret for the {001} face. This selectivity leads to a competition of biuret and urea for the occupation of the empty face sites which slows down the growth on the {001} face. At the same time the adsorption is reversible, thus the incorporation of additive molecules in the growing lattice is avoided. Acetone, which exhibits structural compatibility neither with the {001} face nor with the {110} face has a lower affinity for the urea crystal. Moreover the adsorption of acetone on the two faces is characterized by a moderate difference in free energy. We can therefore predict a negligible effect on the shape of the urea crystals obtained from water solution in the presence of acetone.

The study of the paradigmatic case of urea allowed us to identify some key ingredients that could be used in the design of additives capable of avoiding the formation of needle-shaped crystals. High affinity and high selectivity for the fast growing face of a needle crystal emerged as crucial for a potential shape-affecting effect. These features are inherently related to the structure of the additives that should exhibit moieties capable of reversibly bind the lattice sites exposed on the fast growing crystal face thus limiting its growth rate.

■ ASSOCIATED CONTENT

Ⓢ Supporting Information

Supplementary results discussion, force field charges and GAFF atom types used to parametrize the additives, brief description of well-tempered metadynamics, convergence of the free energy estimations, adsorption FES for biuret, acetone, and urea, and finite size dependence of the growth on the {110} surface. This material is available free of charge via the Internet at http://pubs.acs.org.

■ AUTHOR INFORMATION

Corresponding Author

marco.mazzotti@ipe.mavt.ethz.ch; parrinello@phys.chem.ethz.ch

Notes

The authors declare no competing financial interest.

■ ACKNOWLEDGMENTS

The computational time for this work was provided by the Swiss National Supercomputing Center (CSCS) and by the ETH Zurich Brutus cluster. M.P. acknowledges the European Union grant ERC-2009-AdG-247075 for funding.

■ REFERENCES

(1) Chow, K.; Tong, H. H. Y.; Lum, S.; Chow, A. H. L. *J. Pharm. Sci.* **2008**, *97*, 2855−2877.
(2) Snyder, R. C.; Veesler, S.; Doherty, M. F. *Cryst. Growth Des.* **2008**, *8*, 1100−1101.
(3) Variankaval, N.; Cote, A. S.; Doherty, M. F. *AIChE J.* **2008**, *54*, 1682−1688.
(4) Acquah, C.; Karunanithi, A. T.; Cagnetta, L. E. K.; Achenie, M.; Suib, S. L. *Fluid Phase Equilib.* **2009**, *277*, 73−80.
(5) Oullion, M.; Puel, F.; Févotte, G.; Righini, S.; Carvin, P. *Chem. Eng. Sci.* **2007**, *62*, 820−832.
(6) Kempkes, M.; Vetter, T.; Mazzotti, M. *Chem. Eng. Res. Des.* **2010**, *88*, 447−454.
(7) Weissbuch, I.; Addadi, L.; Lahav, M.; Leiserowitz, L. *Science* **1991**, *253*, 637−645.
(8) Zhang, X. Y.; Fevotte, G.; Zhong, L.; Qian, G.; Zhou, X. G.; Yuan, W. K. *J. Cryst. Growth* **2010**, *312*, 2747−2755.
(9) Fiebig, A.; Jones, M. J.; Ulrich, J. *Cryst. Growth Des.* **2007**, *7*, 1623−1627.
(10) Grimbergen, R. F. P.; Meekes, H.; Bennema, P.; Strom, C. S.; Vogels, L. J. P. *Acta Crystallogr.* **1998**, *A54*, 491−500.
(11) Meekes, H.; Bennema, P.; Grimbergen, R. F. P. *Acta Crystallogr.* **1998**, *A54*, 501−510.
(12) Mougin, P.; Clydesdale, G.; Hammond, R. B.; Roberts, K. J. *J. Phys. Chem. B* **2003**, *107*, 13262−13272.
(13) Pino-García, O.; Rasmuson, Å. C. *Cryst. Growth Des.* **2004**, *4*, 1025−1037.
(14) Vetter, T.; Mazzotti, M.; Brozio, J. *Cryst. Growth Des.* **2011**, *11*, 3813−3821.
(15) Anwar, J.; Zahn, D. *Angew. Chem.-Int. Edit.* **2011**, *50*, 1996−2013.
(16) Davey, R.; Fila, W.; J., G. *J. Cryst. Growth* **1985**, 607−613.
(17) Scott, C.; Black, S. *Org. Process Res. Dev.* **2005**, 890−893.
(18) Jinghua, W. M. Sc. Thesis, ETH Zurich, Zurich, Switzerland, 2012.
(19) Piana, S.; Reyhani, M.; Gale, J. D. *Nature* **2005**, *438*, 70−73.
(20) Piana, S.; Gale, J. D. *J. Am. Chem. Soc.* **2005**, *127*, 1975−1982.
(21) Yani, Y.; Chow, P. S.; Tan, R. B. H. *Mol. Pharm.* **2011**, *8*, 1910−1918.
(22) Zhu, W.; Romanski, F. S.; Meng, X.; Mitra, S.; Tomassone, M. S. *Eur. J. Pharm. Sci.* **2011**, *42*, 452−461.
(23) Aschauer, U.; Spagnoli, D.; Bowen, P.; Parker, S. C. *J. Colloid Interface Sci.* **2010**, *346*, 226−231.
(24) Anwar, J.; Boateng, P. K.; Tamaki, R.; Odedra, S. *Angew. Chem., Int. Ed.* **2009**, *48*, 1596−1600.
(25) Santiso, E. E.; Trout, B. L. *J. Chem. Phys.* **2011**, *134*, 064109.
(26) Trudu, F.; Donadio, D.; Parrinello, M. *Phys. Rev. Lett.* **2006**, *97*, 105701.
(27) Tribello, G. A.; Bruneval, F.; Liew, C. C.; Parrinello, M. *J. Phys. Chem. B* **2009**, *113*, 11680−11687.
(28) Tribello, G. A.; Bruneval, F.; Parrinello, M. *J. Phys. Chem. B* **2009**, *113*, 7081−7085.
(29) Bulo, R. E.; Donadio, D.; Laio, A.; Molnar, F.; Rieger, J.; Parrinello, M. *Macromolecules* **2007**, *40*, 3437−3442.
(30) Metzler, R. A.; Tribello, G. A.; Parrinello, M.; Gilbert, P. U. P. A. *J. Am. Chem. Soc.* **2010**, *132*, 11585−11591.
(31) Xiu, P.; Yang, Z.; Zhou, B.; Das, P.; Fang, H.; Zhou, R. *J. Phys. Chem. B* **2011**, *115*, 2988−2994.
(32) Duffy, E.; Kowalczyk, P.; Jorgensen, W. *J. Am. Chem. Soc.* **1993**, *115*, 9271−9275.
(33) Smith, L.; Berendsen, H.; van Gunsteren, W. *J. Phys. Chem. B* **2004**, *108*, 1065−1071.
(34) Cornell, W.; Cieplak, P.; Bayly, C.; Gould, I.; Merz, K.; Ferguson, D.; Spellmeyer, D.; Fox, T.; Caldwell, J.; Kollman, P. *J. Am. Chem. Soc.* **1995**, *117*, 5179−5197.
(35) Wang, J.; Wolf, R.; Caldwell, J.; Kollman, P.; Case, D. *J. Comput. Chem.* **2004**, *25*, 1157−1174.
(36) Swaminathan, S.; Craven, B. M. *Acta Crystallogr., Sect. B* **1984**, *40*, 300−306.

(37) Mennucci, B.; Cances, E.; Tomasi, J. *J. Phys. Chem. B* **1997**, *101*, 10506−10517.
(38) Bayly, C.; Cieplak, P.; Cornell, W.; Kollman, P. *J. Phys. Chem.* **1993**, *97*, 10269−10280.
(39) Frisch, M. J. et al. *Gaussian 09*, revision A.1; Gaussian Inc.: Wallingford, CT, 2009.
(40) Momma, K.; Izumi, F. *J. Appl. Crystallogr.* **2008**, *41*, 653−658.
(41) Hess, B.; Kutzner, C.; Lindahl, E. *J. Chem. Theory Comput.* **2008**, *4*, 435−447.
(42) Bussi, G.; Zykova-Timan, T.; Parrinello, M. *J. Chem. Phys.* **2009**, *130*, 074101.
(43) M., P.; A., R. *J. Appl. Phys.* **1981**, *52*, 7182−7190.
(44) Kirkwood, J. *J. Chem. Phys.* **1935**, *3*, 300−313.
(45) Laio, A.; Parrinello, M. *Proc. Natl. Acad. Sci. U.S.A.* **2002**, *99*, 12562−12566.
(46) Barducci, A.; Bussi, G.; Parrinello, M. *Phys. Rev. Lett.* **2008**, *100*, 020603.
(47) Barducci, A.; Bonomi, M.; Parrinello, M. *Wiley Interdiscip. Rev. Comput. Mol. Sci.* **2011**, *1*, 826−843.
(48) Allen, T.; Andersen, O.; Roux, B. *Proc. Natl. Acad. Sci. U.S.A.* **2004**, *101*, 117−122.
(49) Roux, B.; Andersen, O. S.; Allen, T. W. *J. Chem. Phys.* **2008**, *128*, 227102.
(50) PLUMED: A portable plugin for free-energy calculations with molecular dynamics, see: Bonomi, M.; Branduardi, D.; Bussi, G. b.; Camilloni, C.; Provasi, D.; Raiteri, P.; Donadio, D.; Marinelli, F.; Pietrucci, F.; Broglia, R. A.; Parrinello, M. *Comput. Phys. Commun.* **2009**, *180* (10), 1961−1972.
(51) Ohara, M.; Reid, R. C. *Modeling crystal growth rates from solution*; Prentice Hall Inc.: Englewood Cliffs, 1973.
(52) Hartman, P.; Bennema, P. *J. Cryst. Growth* **1980**, *49*, 145−156.
(53) Docherty, R.; Clydesdale, G.; Roberts, K. J.; Bennema, P. *J. Phys. D: Appl. Phys.* **1991**, *24*, 89−99.
(54) Vlieg, E.; Deij, M.; Kaminski, D.; Meekes, H.; vanEnckevort, W. *Faraday Discuss.* **2007**, *136*, 57−69.
(55) Berteotti, A.; Barducci, A.; Parrinello, M. *J. Am. Chem. Soc.* **2011**, *133*, 17200−17206.